Declining Global Per Capita Agricultural Production and Warming Oceans Threaten Food Security

Authors:

Chris C. Funk, PhD
U.S. Geological Survey Earth Resources Observation and Science (EROS) Center Department of Geography, University of California Santa Barbara
Ellison Hall, UCSB, Santa Barbara, 96105
cfunk@usgs.gov
(805) 696-9395
(805) 893-3146 (fax)

Molly E. Brown, PhD
NASA Goddard Space Flight Center,
Biospheric Sciences Branch, Code 614.4
Greenbelt MD

Key Words: Global food security, food availability, agricultural production, agricultural development, climate change, drought, population growth

Abstract

Despite accelerating globalization, most people still eat food that was grown locally. Developing countries with weak purchasing power tend to import as little food as possible from global markets, suffering consumption deficits during times of high prices or production declines. Local agricultural production, therefore, is critical to both food security and economic development among the rural poor. The level of local agricultural production, in turn, will be controlled by the amount and quality of arable land, the amount and quality of agricultural inputs (fertilizer, seeds, pesticides, etc.), as well as farm-related technology, practices, and policies. In this paper we discuss several emerging threats to global and regional food security, including declining yield gains that are failing to keep up with population increases, and warming in the tropical Indian Ocean and its impact on rainfall. If yields continue to grow more slowly than per capita harvested area, parts of Africa, Asia, and Central and Southern America will experience substantial declines in per capita cereal production. Global per capita cereal production will potentially decline by 14 percent between 2008 and 2030. Climate change is likely to further affect food production, particularly in regions that have very low yields due to lack of technology. Drought, caused by anthropogenic warming in the Indian and Pacific Oceans, may also reduce 21st century food availability by disrupting Indian Ocean moisture transports and tilting the 21st century climate toward a more El Niño-like state. The impacts of these circulation changes over Asia remain uncertain. For Africa, however, Indian Ocean warming appears to have already reduced main growing season rainfall along the eastern edge of tropical Africa, from southern Somalia to northern parts of the Republic of South Africa. Through a combination of quantitative modeling of food balances and an examination of climate change, we present an analysis of emerging threats to global food security.

1.0 Introduction

Despite accelerating globalization, food security in most of the developing world depends upon local food production. Most rural citizens in developing nations are involved in agriculture (Lamb 2000). Most locally produced goods are consumed locally, so increasing local productivity and slowing population growth remains a central food security issue (Devereux and Maxwell 2001; Schmidhuber and Tubiello 2007). Over the past few years, energy price increases, biofuels, and food scarcity have led to higher global food prices and price volatility[1]. Rapidly increasing consumer prices limit food access. Increased price volatility reduces the benefit that small scale farmers derive from higher producer prices. Biofuels create competition between poor people in the developing world and energy consumers in the developed world. While higher priced commodities can bring direct benefits to farmers, these benefits will not be attained without significant and sustained investments in agriculture to increase production and in programs that reduce price volatility.

High and volatile food prices make local production even more important for food insecure regions. With high prices and continually increasing transportation costs, producing more locally will become an important source of vitality for programs focused on reducing poverty (FAO 2007). The recent entry into small-scale agricultural investment by the Bill and Melinda Gates Foundation has added new vibrancy to efforts focused on understanding barriers to increasing yields and sustaining production in the face of climate change.

This paper explores the convergence of three different trends: changes in agricultural production, changing climate, and increasing population. Our assumption in the analyses presented here is that the fact that some countries have substantially less purchasing power than others will persist over the next several decades. Although global trade is important, we assume that regions with small agriculturally based economies today are unlikely to transform themselves into industrial nations without first improving their agricultural productivity (Kates 2000; Fafchamps 2004; Haggblade 2007). The collision between increasing global food demand, competition for food with developed world energy consumers, and increasingly difficult production conditions means that the food security situation is likely to worsen before it gets better. Climate change will potentially bring reduced rainfall over some regions, and increased rainfall over others. The impact of these changes on agriculture must be anticipated and planned for (Verhagen et al. 2004).

To this end, this paper examines probable trends in per capita cereal production and rainfall. If the current rates of yield and population increases persist, many regions will see substantial declines in cereal availability. Greenhouse gas-induced reductions in monsoonal rainfall could exacerbate these grain shortages. On the other hand, relatively modest yield improvements in the least developed nations could lead to improved levels of per capita cereal production by 2030. If done sustainably, raising yields in these poorest nations may be the most technologically feasible way of addressing global cereal demands while reducing poverty and food insecurity.

[1] Between 2000 and 2007, increased biofuel demand contributed 30 percent of the weighted average increase of global grain prices. Personal communication, Joachim von Braun, IFPRI, October 2008.

2.0 Data

This study uses five sets of data (Table 1): agricultural statistics, population, observed rainfall, and simulated rainfall from 10 different global climate models (Table 2). Based on primitive equations describing the conservation of mass, momentum, radiation, and other key dynamic controls, the global climate models simulate the full atmosphere at ~6 hourly time steps. These models may be constrained by observed sea surface temperatures (SSTs), or run coupled with ocean models in full simulation mode. When constrained by observed SSTs, the models produce circulations resembling the observed atmosphere. We use 24 of these 20th century (1980-2000) simulations from 10 models to examine how well the models recreate observed seasonal rainfall variations between 1980 and 2000 (represented by the GPCP rainfall observations). Our study also examines 21st century CO_2 doubling climate change simulations (Meehl et al. 2007). When coupled to ocean models and forced by projected trends in greenhouse gasses and aerosols, climate simulations can be used to examine the impact due to anthropogenic emissions into the atmosphere. This study examines 28 simulations from a standard emission scenario: the SRESA1B. Under this scenario, atmospheric CO_2 concentrations are assumed to double by 2100.

3.0 Methods

We describe below the approach taken by our regional food balance trend analysis, our analysis of climate change scenarios, and our detailed analyses of Eastern African food security projections.

3.1 Regional food balance projections

One basic tenet of our work is that food availability plays a critical and increasing role in food security. Following the UN's Food and Agriculture Organization's division of the world into 18 regions[2], and using 1961-2007 data on total cereal yields, harvested area, and total population, we can write a simple equation describing per capita cereal production (c, [kg per person per year]) in terms of total harvested area (a,[hectares, 1 ha = 100 m x 100 m]), total population (n, [people]), and total annual cereal yields (y, [kg per ha per year]).

$$c = \frac{a \cdot y}{n} \qquad \text{eq. 1}$$

Per capita cereal production (c) is a large region, a is harvested area in hectares (1 hectare = 100 m x 100 m), n is the total population, and y is annual yield expressed in kilograms per hectare.

This is a coarse metric that clearly ignores many important food security variables related to nutrition, access, trade, vulnerability, pastoral livelihoods, etc. (Davis et al. 2001; Devereux and Maxwell 2001). Nonetheless, per capita cereal production is an important indicator of food availability, especially in large landlocked regions with large agrarian populations. This restriction applies to most of Africa, Asia, and Southern America. We examine FAO statistics averaged over very large multi-national regions, and this tends to diminish the relative impact of cross-border trade. Another advantage of this approach is transparency. We can examine trends

[2] http://unstats.un.org/unsd/methods/m49/m49regin.htm

in per capita harvested area and yields and diagnose their relationship to per capita agricultural production, analyzing shifts in agricultural production and baseline vulnerability.

Conceptually, per capita production can be divided into 'pessimist' and 'optimist' tendencies (Fig. 1); Per capita harvested area declines while yields increase. Since 1961, in almost all regions of the world, the population (n) has grown faster than the harvested area (a), so that the per capita planted area decreases with time. Per capita harvested area thus represents the interaction of finite environmental resources with an expanding population. Other related factors, such as land degradation and soil nutrient depletion, are likely to operate in the same limiting sense (Blaikie and Brookfield 1987).

Yield trends, on the other hand, denote increases in human knowledge, innovation, social and economic organization, as well as the ability and willingness to invest in improving agricultural production (Lo and Sene 1989; Watts 1989; Turner et al. 1993). Yield trends everywhere in the world, have been positive over the past 50 years (Cassman et al. 2003). Together, per capita harvested area and yield trends describe the direction of per capita cereal production, one major determinant of food security.

Our focus is not on identifying individual food crises but on exploring slow changes in agricultural sustainability. Therefore, for this study we have used 10 year averages of and for the 1960s, 1970s, 1980s, 1990s, and 2000-2007. Denoting trends with over-arrows, we can express approximate tendencies in per capita cereal as a function of time.

In order to better grasp the human impacts of shifting relationships between population and cereal production, we define a 'theoretical population without food' or p.

$$p = [(ay) - (ng)]\ g^{-1} \qquad \text{eq. 5}$$

In this equation, p is the theoretical population without food, measured in units of people, (ay) is annual cereal production [kg per year], and g is the annual grain requirement per person [kg per person per year]. In practice, g varies substantially between cultures and livelihood groups. In this study, we assume a caloric requirement of 1,900 calories and typical caloric content of 3,600 calories per kilogram of grain. This leads to an annual grain requirement, in theory, of 190 kilograms of grain per year. This calculation, of course, presumes a perfect distribution of grain, and no use of cereal for biofuels, livestock, alcohol, or other purpose (Pech et al. 2005, Cassman 2007). On the other hand, it also ignores imports and other sources of nutrition. While only a rough approximation of food availability, equation 5 gives us a means of approximating the magnitude of cereal deficits and surpluses. Regions experiencing large cereal deficits may have theoretical food balances with large negative values, indicating that millions of people may experience food shortages. On the other hand, some regions may have large grain surpluses, capable, in theory, of supporting millions of people. It is important to note that this calculation assumes a low baseline consumption rate.

3.2 Climate Change Rainfall Projections

Because global climate models represent terrestrial rainfall poorly, it is often preferable to focus on how large scale climate features that they represent well. Two such patterns are rainfall over central Indian Ocean (IO) and the 1st principal component (PC1) of global seasonal precipitation. We describe these indicators, evaluate how they might change during the early 21st century, and use these changes to predict 2050 shifts in mean rainfall.

The central Indian Ocean is a critical driver of drought along the eastern seaboard of Africa (Verdin et al. 2005). Greenhouse gas emissions have led to a much warmer Indian Ocean; this warming disrupts onshore moisture transports into Southern and Eastern Africa, substantially reducing main season rainfall, especially during the six months between December and May (Funk et al., 2008). In this study, we use seasonal March-April-May (MAM), June-July-August (JJA), September-October-November (SON), and December-January-February (DJF) rainfall totals averaged between 0-15°S and 60-90°E to represent Indian Ocean warming. We refer to this indicator as 'IO,' for 'Indian Ocean[3]'.

Variations in the tropical Pacific Ocean also drive global changes in precipitation. The most important time variations of global rainfall anomalies can be summarized by their 'principal components', or PCs, which are time series designed to succinctly summarize the underlying data. The first principal component of global rainfall (PC1) is strongly correlated with El Niño and tropical SSTs in the central-eastern tropical Pacific.

[3] Please note that this indicator is distinct from the Indian Ocean dipole, which compares sea surface temperature (SST) anomalies in the southeastern and northwestern tropical Indian Ocean.

In this study we briefly examine the IO and PC1s from a large set of climate change simulations (Table 2). Using historical observations, we then statistically link variations in our two indicators with variations in observed terrestrial rainfall. These hybrid dynamic-statistical models rely on the climate models to predict the changing behavior of large scale climate features. They rely on statistics to interpret the local implications of these changes. Two hybrid statistical-dynamic reformulations are presented: a global reformulation (Brown and Funk, 2008) and a higher resolution analysis focused on eastern and southern Africa.

Note that this hybrid statistical-dynamic technique is quite distinct from the evaluations provided by the IPCC (Solomon et al. 2007). Our statistical downscaling approach tends to identify declines in monsoonal precipitation in Asia and Eastern Africa, where the IPCC simulations tend to suggest increasing rainfall.

3.3 Detailed analysis of Eastern African food aid tendencies.

We will then present a more detailed discussion of food security tendencies in Eastern and Southern Africa. Specifically, we analyze Eritrea, Ethiopia, Kenya, Uganda, Rwanda, Burundi, Tanzania, Zambia, Malawi, Mozambique, Zimbabwe, Swaziland and Lesotho. This region broadly aligns with the FAO's 'Eastern Africa' region (FAO 2007). Climatically, this collection of nations along the eastern edge of Africa falls into two groups. The southern states experience a single rainfall maximum during the December-February (DJF) season. The northern states, in the Greater Horn of Africa, typically experience two rainfall maximums: maxima one, MAM and the other during SON. Ethiopia and Eritrea have a JJA maximum. We have included Tanzania within Southern Africa because DJF is the most agriculturally productive season.

The objective of the analysis is to estimate the relationship between main season rainfall, agricultural statistics, population figures, and World Food Program food aid totals for each of these nations over the 1979-present time period. Log-linear empirical models of national annual cereal production were created by regressing historical FAO production figures against main season rainfall, harvested area, and seed, and fertilizer inputs.

$$p = b_1 r + b_2 a + b_3 s + b_4 f \qquad \text{eq. 6}$$

Where r is main season rainfall expressed as a percent of the historical mean, a is harvested area, s is input seed, and f represents fertilizer use; p is total cereal production [kg], and $b_{1..4}$ are coefficients determined by regression between the natural logs of p, r, a, s, and f. Seed and fertilizer statistics, again obtained from FAO, are measured in kilograms per year. Combining this equation with equation 1 allows us to separate the primary environmental variation (rainfall) from 'structural' components of national per capita cereal production.

$$c = b_1 r + b_2 a + b_3 s + b_4 f + \pi \qquad \text{eq. 7}$$

In this equation c is per capita cereal production [kg per person per year]. This expression is similar to equation 1, but more explicit. The key factors controlling yields (seeds, fertilizer and rainfall) are now included. This gives us a quantitative means to diagnose the impacts of drought

and changes in seed and fertilizer use. We can further separate equation 7 into an environmental portion (e) and human (h) components.

$$c = eh$$
$$e = b_1 r$$
$$h = (b_2 a \cdot b_3 s \cdot b_4 f \cdot n^{-1}) \quad \text{eq. 8}$$

The environment component contains interannually varying weather, plus perhaps long-term variations that may be associated with climate change. The human component encodes a combination of population (n) and large-scale agricultural controls (harvested area a, seed use s, and fertilizer use f, as per capita demand based on population. We refer to this combination of factors (h) as 'per capita agricultural capacity'. Typically, all of these terms tend to trend strongly and vary less than rainfall on interannual time scales. Thus, agricultural capacity trends tend to dominate food security variations on decadal time scales. Rainfall tends to vary substantially from year to year, producing variations in production about a baseline.

For Eastern, Western, and Southern Africa, the inverse of national per capita cereal production (i.e., a food deficit or imbalance) is strongly related to regional, decadal variations in WFP food aid (R^2=0.87, Funk et al., 2008). Area harvested trends, seeds, fertilizer, and population may be placed in equation 8 to assess the potential impacts these tendencies have on baseline agricultural capacity. The relative impact of rainfall versus structural elements may be assessed via equation 8. Equation 8 implies a potential for multiplicative impacts in areas experiencing both drought and decreasing per capita agricultural capacity.

4.0 Results

4.1 Global food balance analysis

Between 1961 and 1986, global total cereal yields increased 89 percent, harvested area expanded 11 percent, and global per capita cereal production increased enormously, peaking around 1986 (Fig. 2). Population, meanwhile, grew by 60 percent over those 25 years, resulting in an increase in per capita cereal production from 284 to 372 kg of grain per person per year. The last 21 years (1987-2007) have seen slower population growth (a 34 percent increase) accompanied by slower yield improvements (a 31 percent increase) and a 2 percent reduction in the total area harvested. Surprisingly, according to FAO and UN statistics, per capita harvested area and fertilizer, and seed use have all declined by 20-30 percent (Fig. 2). Presumably, higher yielding seeds, double cropping of rice, irrigation, and more effective farming techniques have made up for lower per capita inputs. Per capita production stands now at about 350 kg of cereal per person per year, 6 percent below the 1986 peak.

The relative stabilization of global per capita production masks the increased use of cereals for biofuels, alcohol, and meat production, as well as significant variations between regions. Population growth rates vary tremendously geographically (Table 3). Four regions have more than doubled their population since 1980: Eastern Africa, Western Africa, Middle Africa, and Western Asia. Central America, Southern America, Northern Africa, Southern Africa, Southern

Asia, and Southeastern Asia have seen their populations increase by more than 50 percent. Since 1980, two out of every three people born now live in Asia. Another one out of four lives in Africa.

Across most of Africa, harvested area has increased substantially more than yields (Funk et al., 2008). In Eastern Africa, for example, yields have only increased by 25 percent since 1980, while harvested area increased by 55 percent. In Western Africa yields increased by 42 percent while harvested area increased by 127 percent. Yields, per capita harvested area, and production remain very low. Across much of the rest of the world, harvested areas have remained fairly steady, and yields have been the primary driver of agricultural growth. Our evaluation of FAO statistics shows that Southern America, Northern America, Eastern, Southern and Southeastern Asia have experienced greater than 70% increases in yields since 1980. Today, huge regional disparities in yields remain the norm. In 2007, cereal yields varied by almost 600 percent, from ~1,000 kilograms per hectare in Middle Africa, to more than 5,000 kilograms per hectare in Northern America, Eastern Asia, and Europe[4].

Given that global and regional tendencies in per capita harvested area and yields appear fairly predictable (R^2>0.8) at decadal scales (Fig. 1), we may plausibly use the observed trends to project to 2030. Table 4 presents the anticipated 2007 to 2030 changes, expressed as kilograms of cereals per person per year, and as percent changes compared to 2007. Figure 3 shows the historical and projected per capita cereal production for selected regions. Globally, we may anticipate a return to per capita production levels similar to those in the late 1960s, when per capita production was near 327 kg per person. Eastern Asia may return to 1980s production levels (near 300 kg person^{-1}) and Southern Asia to 1960s levels (near 200 kg person^{-1}). Declines in heavily populated Asia could re-expose millions of people to chronic undernourishment[5]. Central and Southern America may experience 18-20 percent declines in per capita cereal production levels. Eastern and Middle Africa, however, may be hit hardest of all, with more than 30 percent reductions in already low per capita cereal production levels, with Eastern Africa going from 131 kg per year in 2007 to 84 kg per person per year in 2030. United Nations (UN) projections suggest that the population of Eastern Africa will increase by 191 million people by 2030—a net increase second only to Southern Asia.

While imprecise, it is instructive to evaluate simple food balance equations, looking at the number of people who could be reasonably supported by the anticipated levels of grain production (Table 4). We do this by calculating the theoretical population without food (equation 5). Globally, our 2030 food balance estimates suggest that as today, we will still have enough grain to maintain our human population, albeit at a low baseline value of 1,900 calories a day. This estimate, however, does not take into account grain consumption associated with livestock consumption, biofuels, or industrial applications.

Most of the production increases supporting these surpluses may occur in Eastern and Southern Asia and Northern America, where our modeling suggests 47 percent and 28 percent of new

[4] Note that this study uses FAO cereal yields data. The specific commodities will vary substantially by region.

[5] Note that due to a short historical archive, we have not modeled central Asia (Kazakhstan, Kyrgyzstan, Tajikistan, Turkmenistan, and Uzbekistan). This region is likely to exhibit similar trends in food security, potentially further exacerbated by increasing temperatures and water scarcity.

production will occur, driven by 25 to 35% increases in yields. Our projected yields in Eastern Asia and Northern America reach 7,500 kg ha^{-1}. Yields of this magnitude assume further innovation and increasing petrochemical inputs, and may be technically infeasible (Cassman et al., 2003). However, regionally, a continuance of recent trends that include vast disparities of access to food will likely expose hundreds of millions more people to chronic food insecurity, even if we ignore increasing cereal demands driven by biofuels and increased consumption.

With a 2030 population on the order of 2.1 billion, Southern Asia will face substantial food availability challenges. Our 2030 projections suggest a per capita cereal production of 193 kg per person per year (Table 4). This level is slightly above our semi-arbitrary subsistence threshold of 190 but substantially (38 percent) below the 2007 value of 231. Hence, while our theoretical 'food balance' suggests sufficiency, real conditions will likely result in chronic food shortages for large segments of this diverse region who have negligible purchasing power. By 2050, our theoretical food balance (equation 5) suggests that regional cereal production might only be adequate for 90 percent of the population, leaving a shortfall equivalent to the consumption of 373 million people. Substantial water scarcity intensified by anthropogenic increases in air temperature and evaporation (Parry et al. 2007), will further hamper agricultural expansion. Central Asia appears likely to face challenges[4] similar to those of Southern Asia.

Africa, especially Eastern and Western Africa, where cereal crops provide the majority of calories, will face substantial and increasing food security challenges. Per capita cereal production in Eastern Africa may decrease from a low 131 kg per person per year in 2007 to a very low 84 kg per person per year in 2030. This decline almost triples the theoretical food imbalance from -96 million in 2007 to -277 million people in 2030. This corresponds to 32 percent of the total population in 2007 and 56 percent of the population in 2030. Western Africa faces a similar, albeit more modest, decline in per capita production (from 189 to 166 kg per person per year). Our theoretical food balance suggests that this could expose about 61 million people, or 14 percent of the population to chronic food shortages.

In this analysis, Africa and Asia emerge as likely foci for continuing decreases in food availability and security. Rapidly growing populations and increasing temperature will place further demands on scarce water supplies. Biofuels and rising demand by the global middle class will likely compete for global production, raising prices and reducing food access for rural and urban poor. Eighty-eight percent of the 2007-2030 population growth will occur in African and Asian countries which will be strongly influenced climatically by the rapidly warming Indian and Pacific tropical Oceans (Funk et al., 2008, Brown & Funk, 2008). We now turn our attention briefly to potential anthropogenic changes in these climate indicators.

4.2 Climate Change Analysis

4.2.1 Potential climate changes in the IO and PC1 climate indicators

What do global climate change models tell us about 21st century rainfall? The models (Table 2), on average, tend to suggest increases in tropical rainfall over the Indian Ocean and tropical Pacific Oceans (Fig. 4). In these regions with very warm surface waters, there is a tight coupling between SSTs and tropical atmospheric dynamics. Future warming of the oceans appears likely to create increased rainfall over the tropical Indian and Pacific basins. This increased oceanic rainfall will release large amounts of energy into the atmosphere, impacting global and regional circulations. We can quantify the magnitude of these impacts by using the 21st century climate change simulations to calculate the PC1 and IO climate indicators (see Section 3.2).

In general, the areas of increasing precipitation (blue areas in Fig. 4) correspond positively, to the geographic footprint of both PC1 and IO, and the suite of models examined suggests that both PC1 and IO will increase by 2050 (Fig. 5). The global (PC1) response, which corresponds strongly to warming the central Pacific, appears to strengthen in all seasons. The IO warming appears much stronger during March-April-May (MAM) and December-January-February (DJF) than June-July-August (JJA) or September-October-November (SON). There is an inherent uncertainty in all these projections however, due to differences in model formulations, natural decadal variations in the climate, and the imperfect simulations of key processes, such as El Niño. We can attempt to quantify this uncertainty by looking at the differences between the simulations. The lines on Fig. 5 show the 68% confidence intervals obtained from these differences. In summary, the models appear to agree on substantial increases in the PC1 and IO indicators, implying associated changes in the Indian and Pacific Oceans circulations, but there is still a high level of uncertainty as to the actual magnitude of the changes.

When dealing with climate change simulations, it is very important to realize how poorly these models tend to represent rainfall over land. The top panel of Fig. 6 shows the average seasonal correlation between 1980-2000 observed and modeled rainfall. Each grid box shows the correlation for the season (DJF, MAM, JJA, SON) with the highest mean rainfall. In general, areas over the tropical oceans are handled well by the climate models, and have reasonably high correlations. In the Indian and Pacific Oceans, these areas also tend to be areas showing substantial increases in rainfall (Fig. 4). The situation, however, is quite different over the land areas. In almost all these areas, historical evaluations suggest very low levels of correlation ($r < 0.3$). This low level of skill makes climate change analysis of 'raw' climate change rainfall simulations problematic. The next section present an alternative approach, based on hybrid-dynamic-statistical reformulations.

4.2.2 Hybrid dynamic-statistical reformulations of 21st century climate change simulations

Hybrid dynamic-statistical reformulations (Funk et al., 2008; Brown and Funk, 2008) provide one potential way to work around the limitations of global climate models. Instead of using the climate model precipitation directly, we use regression (based on historical data) to relate

changes at some location to large scale climate indicators (such as PC1 or IO, Fig. 5). This is especially useful when we have strong prior evidence linking changes in tropical oceanic rainfall and SSTs to terrestrial rainfall. The bottom panel of Fig. 6 shows such precipitation reformulations for the globe (Brown and Funk, 2008), based on the 1st and 2nd principal components of global precipitation. This approach suggests that substantial rainfall declines may appear over Central America, northern South America, Africa, and parts of Southern Asia, and Australia.

For more detailed spatial analysis, we can use regressions between African rainfall and PC1 and IO time-series to downscale anticipated 21st century shifts in these climate forcings. These results are shown in Fig. 7. The season with the highest mean rainfall was selected (left panel, Fig. 7). Regression equations linking PC1 and IO to the local rainfall were then estimated. For most areas, these models explained between 40 and 70 percent of the variance. For parts of sub-tropical Eastern Africa and Southern Africa near the Indian Ocean, increasing IO and PC1 values are associated with increasing aridity; warm anomalies in the south-central Indian Ocean and moderate-to-strong ENSO events are typically associated with below normal MAM or DJF rainfall. These historical relationships, combined with projected increases in the IO and ENSO-like PC1 indicators (Fig. 5), suggest continued declines in rainfall across southern Ethiopia, Somalia, Kenya, northern Tanzania, southern Mozambique and southern Zimbabwe. While considerable uncertainty remains, it appears plausible, and even likely, that portions of Zimbabwe, Mozambique, Tanzania, Kenya, Somalia, and southern Ethiopia may experience greenhouse gas induced rainfall reductions over the next 40 years. If warming the Pacific and Indian Ocean continues, as suggested by climate change models (Fig. 4), anthropogenic drought appears likely to impact one of the most food insecure regions of the world.

Our conclusions are generally in agreement with the most recent 4th IPCC finding that semiarid Africa may experience large-scale water stress and yield reductions by 2020 (Solomon et al. 2007). Our work, however, avoids the direct use of terrestrial precipitation simulations due to their low accuracy (Fig. 6a). Focusing on downscalings (Fig. 7) of climate forcing diagnostics (Fig. 5), however, suggests further drying, especially for Eastern Africa, where the IPCC report (Solomon et al. 2007) suggests that precipitation will increase. Future expansion of this work into Asia could help confirm the potential decline in the Asian monsoon suggested by our global reformulations (Fig. 6b).

4.3 Detailed African Food Security Analysis

In Africa, the trends driving food security evolve in a complex landscape. In Table 5 we show selected agricultural, food aid, and population statistics for 18 semiarid food insecure countries in Western Africa, Eastern Africa and the eastern part of Southern Africa. Data for Ethiopia and Eritrea were combined, as they were united before 1993. Geographic variations between these three regions play a strong role in their level of agricultural self-sufficiency. In 2005, the Western African countries had, on average, three times as much harvested area as Eastern Africa (0.26 versus 0.08 ha person^{-1}). Per capita harvested areas for southeastern portions of Southern Africa are only slightly higher than Eastern Africa (0.10 ha per person^{-1}). There are also considerable differences in per capita harvested area between the countries in each of these regions.

For these countries, harvested area largely determines national cereal production totals[6]. Over the period 2001-2005, the relatively food secure Sahelian countries[7] have per capita agricultural capacity values (h, equation 8) above 190 kg person^{-1} year^{-1}. Over the same period, the southeastern Africa and Greater Horn countries had agricultural capacity values of 122 and 99 kg person^{-1} year^{-1}, respectively. Seed and fertilizer inputs are limited. In 2005, fertilizer inputs were typically below 20 kg ha^{-1} in these low productivity zones.

Low yield growth combined with declining per capita harvested area has led to decreases in per capita agricultural capacity (Table 5). Because of increases in population, these food insecure countries in Eastern, Southern and Western Africa have experienced, respectively, 18, 22, and 28 percent reductions in per capita harvested area between 1979 and 2005. Between 1979 and 2005, per hectare fertilizer increased in the Sahel and Greater Horn and declined in eastern Southern Africa. Of the four main users of fertilizer in 2005, Kenya had increased its fertilizer use from 21 to 67 kg ha^{-1}. Zambia, Zimbabwe, and Swaziland saw substantial reductions from the early 1980s.

In these semiarid countries, a strong dependence on rain-fed smallholder farming practices results in quasi-linear relationships between seasonal rainfall, grain yields, and food deficits. Hence, the agricultural capacity multiplied by rainfall (equation 7) is strongly related to per capita production. The inverse of this measure (food imbalance) is related to food aid. For each country, the food imbalance measure was regressed against 1979-2005 WFP humanitarian assistance. This gives us a pragmatic means of translating changes in rainfall, cropped area, seed use, and fertilizer use into an index of potential food aid requirements, grounded empirically by historical aid figures. Due to the low per capita production, the resulting model performed well at a regional scale for Eastern and Southern Africa ($r=0.86$, $p=1.6\times10^{-5}$) but was less accurate for the Western African countries ($r=0.48$, $p=4.8\times10^{-2}$). We can also express agricultural sufficiency as a theoretical food balance, based on an assumed annual cereals requirement of 190 kg per capita. Changes in the theoretical food balance (equation 5) agree strongly with changes in WFP food aid[8], explaining 70% and 85% of their variance at national and regional scales.

Combining observed 1994-2003 agricultural capacity trends with our projected rainfall tendencies, we can use the model to project 2000 to 2030 food aid requirements (Fig. 8). We show historical WFP aid figures, historical model aid figures, and results from four sets of aid projection scenarios. The first scenario assumes that recent trends in population, rainfall, crop area, seed use, and fertilizer use continue for the next 30 years. The second scenario is the same, but with the change in rainfall inferred from our 1950-2005 Indian Ocean regressions and 21st century climate simulations. The third scenario assumes that precipitation levels will remain similar to those observed today. The fourth is an 'agricultural growth' scenario, in which observed rainfall trends continue, but per capita food availability is assumed to increase by 2 kg per person per year.

---

[6] $R^2=0.96$ for 1979-2005 mean area vs. production totals for these 18 countries.

[7] Sparsely populated Mauritania and groundnut-dependent Senegal are not well modeled in this analysis structure.

[8] We admit to a certain circularity of argument here. FAO food balance calculations have been used to guide WFP aid distributions, helping to enforce a tautological relationship. The data we choose to collect often follows closely our pre-existing observations, and tend to follow our theoretical paradigms (Kuhn 1962).

These results suggest that the interaction between drought and declining agricultural capacity (which includes population growth) may be explosive, dangerous, and costly, with annual aid totals increasing by 83 percent by 2030. The 'observed' versus 'projected' trends differ primarily for the Sahel (Fig. 8). The impact of climate change on the Sahel is keenly debated, and our analysis explicitly ignores influences from the Atlantic Ocean. Current agricultural capacity and rainfall trends will likely produce a 60 percent increase in food aid expenditures in the next two decades, and will likely lead to a 43 percent increase in food insecurity in Africa. These figures are significant because food aid is a proxy indicator for a host of related problems including child malnutrition, as well as declines in health, productivity, and economic growth (FAO, 2007). Including limitations in growth of harvested area and the impacts of increased growing season temperatures and potential evapotranspiration would inflate all these aid projections. Two hundred million sub-Saharan Africans were undernourished in 2002, and if the observed 1982-2002 trend continues this total may climb to almost 600 million people by 2030.

4.4 World Yield Analyses

We conclude by presenting graphically (Fig. 9), a set of projected and target agricultural yield values for the FAO regions. The projected yields are those based on 1961-2007 linear trend models. Annual yield trends vary significantly by region. North America, Western Europe, and Eastern Asia have seen increases of over 700 kg ha^{-1} $annum^{-1}$. Projections (Fig. 9a) for some of these regions in 2030 reach beyond 7,000 kg ha^{-1}. These projected yields may be beyond practical limits (Cassman et al. 2003). Western, Middle, and Eastern Africa, conversely, have exhibited very slow growth in yields (Table 5), with annual changes in yields of less than 110 kg ha^{-1} $annum^{-1}$. Without accelerated agricultural development, 2030 yields will still be very low.

Figure 9a also shows the anticipate 2007 to 2030 transition in per capita production [kg $person^{-1}$ $annum^{-1}$]. The 2007 value in kg per person per year is shown to the left of the arrow, the 2030 prediction is shown to the right.

Substantial reductions appear likely for Southern and Central America, Western and Eastern Africa, and Southern and Eastern Asia. Middle Africa and central Asia may exhibit similar tendencies but were not modeled due to data limitations. Projected 2030 yields in Central America, Western and Eastern Africa, and Southern Asia remain low, below 4,000 kg ha^{-1} $annum^{-1}$.These two scenarios contrast 'business as usual' outcomes with plausible agricultural growth patterns. In the former, future yield trends are assumed to be the same as 1961-2007 yield trends (Table 3). In the latter scenario, we set baseline per capita cereal production targets and solve for the necessary yields in 2030.

The 'business as usual' projected yields analysis (Fig. 9a) displays three key characteristics: i) yield trends and 2030 yield outcomes vary dramatically by region, ii) in developed nations a continuance of observed yield trends may result in physically unrealistic results, and iii) in Africa, Central America and Southern Asia, a continuance of current trends will result in very low levels of food availability. Given increasing globalization and technological limits, one might imagine that yields would have converged since 1960. This has not been the case; rather the green revolution has followed a course in which the 'green get greener', with growth then

slowing above 5,000 kg per ha per year. Yields in 1961 have been a very good predictor of yields in 2007 (R^2=0.8.6); countries with lower yields have tended to increase their yields more slowly. This has enhanced differences between nations. In 1961 the highest regional yields were four times the lowest. This ratio rose to nine in 2007. A continuance of these trends will increase this ratio to 11 by 2030. As yield growth lags and per capita harvested areas decline, per capita cereal production will reach dangerous levels in Africa, Central America and Southern Asia.

As an alternative to using observed yield trends from Table 3, we can specify a target 2030 per capita production and solve directly for the required yield (Fig. 9b). This approach uses trends in per capita harvested area but then estimates 2030 yields algebraically. Two sets of cereal production targets were used. A minimal threshold of 190 kg ha^{-1} $annum^{-1}$ was specified for African nations. The other countries were set to their 2007 values. This represents a modest 'agricultural growth' scenario, in which per capita production for most of the world maintains parity with current levels and Africa experiences modest gains.

This exercise suggests two salient results. First, the target yield gains for Africa appear small in magnitude but large in ratio. Looking at Eastern Africa, for example, we see that a transition from yields of 1,482 kg per hectare per year (Table 3) to 3,500 kg per hectare per year (Fig. 9b) would make the region relatively food secure. This is a large percent increase, but not technically impossible – farming efficiencies would have to approach those used in Southern America in 2007 (Fig. 9a).

A second salient feature of Fig. 9b is that maintaining current per capita cereal production levels in Northern America and Eastern Asia will require substantial increases in yields, well beyond those anticipated by historical trends. As per capita harvested area diminishes rapidly in these regions, very large increases in yields will be required to produce enough cereal to feed the future population at its current level of per capita cereal consumption. In order for Eastern Asia to maintain a per capita cereal production of 314 kg per person per year, yields will have to increase from their 2007 level of 5,418 kg per hectare per year (Table 3) to a very high yield of 8,600 kg per hectare per year. This may not be technically feasible or environmentally sustainable.

Although there is a substantial gap between maximum theoretical yield for the major world crops of maize, rice, and wheat and actual average yields, in recent years the gains in yields have declined. Rice yields in China and Indonesia and wheat yields in India and France, for example, have not increased substantially in the past decade (Cassman et al. 2003). Increasing yields beyond levels attained in these countries will require either enormous investments in freshwater irrigation systems or a transformation of the agricultural systems to incorporate new technological advancements, both of which are highly unlikely in the next few decades. Investing in regions with extremely low agricultural productive capacity, therefore, will be a much less expensive way to improve global agricultural production. Bringing maize yields from 700 to 5,000 kg per hectare is far easier than increasing yields from 7,000 kg per hectare to 8,000 kg per hectare (Naylor 1996). This observation turns the standard food security paradigm on its head. With lower population growth and more effective farming practices, by 2030 it could be an agriculturally active Africa that helps alleviate global shortages of cereal production.

5.0 Conclusions

Food security and agricultural production are not directly linked. Politics, economics and access are also critical issues. In countries that experience significant levels of hunger, however, productive capacity is an important constraint, made more salient by increasing food price volatility. Investment in further productive capacity in regions with growing populations remains a challenge. This paper has presented analyses that show that without concerted effort, today's food security crisis will continue to accelerate, robbing millions of people of their potential livelihoods. Our results suggest that large-scale trends in yields and per capita harvested area (Fig. 2) are very predictable. We can be quite certain that the world will experience significant reductions in food availability as consumption demands increase due to biofuels and rising living standards.

Some parts of the developing world, like Southern Asia, may have 2030 per capita production levels similar to those of the 1960s or 1970s (Fig. 3). Other regions, such as Eastern Africa, face burgeoning food crises if current trends persist (Fig. 9). Greenhouse gas induced warming in the tropical Indian Ocean (Funk et al. 2008) and Pacific Ocean (Brown and Funk 2008) could exacerbate the likelihood of drought across many food producing regions (Figs. 6 & 7). Anthropogenic drought appears quite likely to affect chronically insecure Eastern Africa. In Kenya, the 2007 and 2008 long and short rains appear to be the worst since 1979 (Funk and Verdin, 2009). Our food balance modeling (Fig. 8), however, suggests that agricultural development is likely to be a reasonable and effective mitigation strategy. The alternative may be a continued and expensive increase in chronic food aid.

Less certain but plausible climate change impacts on Southern Asia could also threaten agricultural production. Anthropogenic drought in Southern Asia (Fig. 6b), combined with declining per capita harvested areas, could lead to an explosive decrease in cereal availability, below the return to 1970 levels anticipated by our trend analysis (Fig. 3).

Many trends affect agricultural sustainability. It is important to recognize the complexity and interaction of these different factors. At the farm level, land modifications, plot landscape positioning, alternative crops or varieties, in-soil vegetative material, and well-placed biodiversity can all play a role in countering unfavorable climatic events. Degradation in soil quality and in the overall natural resource base may threaten the long-run viability of several of the world's most intensive agricultural systems. Combined with monocultures of improved crops supported through high levels of inputs, much can be done to increase agricultural productivity in regions that currently produce 10 percent or less of their theoretical potential (Brown and Funk 2008). Agricultural innovations require political and economic stability, investment, and societal learning that must be sustained over relatively long periods. Some places in the developing world have managed to capitalize on new techniques and technology to significantly increase production, such as in Kenya's main maize growing districts where maize yields have increased from 3,000 to 5,000 kg per hectare in the past eight years[9]. These gains are threatened when national political crises cut off roads, restrict access to critical inputs, and cause uncertainty

[9] Personal communication, Curt Reynolds, August 2008.

in export contracts. The context in which production occurs is just as important as production itself.

Economic growth, improved food security, and wide-scale poverty reduction all require productivity gains in agriculture (Haggblade 2007). Agriculture serves as a powerful engine of poverty reduction, one which can bring the poorest a rapid improvement in income through direct technology transfer. According to Michael Lipton, "no country has achieved mass dollar poverty reduction without prior investment in agriculture" (Lipton 2005). Available evidence suggests that investment in public goods such as agricultural research, agricultural extension, and road networks constitutes one of the most effective tools available for stimulating economic growth and poverty reduction. Increasing per capita agricultural production in regions that currently have very low yields can be achieved with investment in these public goods (Platteau 1996, Lamb 2000). These investments can result in significant gains in incomes, and reduction in poverty, which will reduce the number of people chronically malnourished.

Improved economic development, aid, and agricultural policies, backed by adequate resources, can prevent humanitarian crises. Improved agricultural capacity is one of many reasonable ways we can reduce vulnerability within Africa. Improved seed and fertilizer distribution can enhance yields, as can better land tenure and management policies. Expensive and potentially disruptive food aid shipments are much smaller than domestic African crop production. Since local cereal production is 100 times greater than food aid totals, modest increases in African food production could eradicate food production shortfalls. Our food balance modeling (Figure 8), suggests that modest increases in yield would help eliminate the need for most external shipments of food aid.

Acknowledgements: The authors would like to sincerely thank our anonymous reviewers, as well as colleagues from the USGS who graciously supplied their comments. Without their efforts this paper would be much less coherent. We would also like to express our gratitude to the UN Food and Agricultural Organisation and the Program for Climate Model Diagnostics and Intercomparison for providing, respectively, access to the agriculture and climate modeling data used in this study. This research has been supported by funding from the US Agency for International Development Famine Early Warning System Network, the NASA Precipitation Monitoring Mission (grant NNX07AG26G), and a NASA decision support project (Cooperative Agreement Notice NN-H-04-Z-YO-010-C).

Figure and Table Legends

Table 1. Sources of agricultural, social and climate data used in this analysis.

Table 2. Number of 20th century[a] (1980-2000) & 21st century[b] (2000-2100) simulations used in this study. These model simulations are produced by premier climate modeling groups[c] in the United States, Europe and Asia.

Table 3. This table shows relevant agricultural statistics for 2007 obtained from the FAO. Unless international trade and aid can make up the difference, areas with theoretical food balance deficits will face systematic food shortages. The magnitude of these shortages can be evaluated by looking at the food balance deficits expressed as percentages of the total population. With some exceptions, regions with the largest population increases over the past 27 years also have the largest per capita food deficits.

Table 4. Global and regional projections of per capita cereal production (equation 1) and theoretical food balance (equation 5) statistics. These values were based on 2030 estimates of yields and per capita harvested area. Overall, and on average for the world, there will be 48 kg less of cereal production per person per year in 2030, a 14% reduction over the 354 kg per person produced in 2007.

Table 5. Selected African agriculture and population statistics from the FAO.

Fig. 1 Oberserved (FAO) and modeled global cereal trends in per capita harvested area and yields. Data values have been averaged by decades. The filled circles show observed global cereal yields. Decadal increases in global yields are fit very well by a linear trend model (filled circles). The open boxes show observed per capita harvested area decreases. Decadal decreases in global per capita harvested areas are also fit very well by a linear trend model (filled boxes). The relative rates of yield increases and per capita harvested area decreases can be used to predict future per capita cereal production.

Fig. 2 Global per capita cereal production statistics, expressed as fractions of a 1986 baseline. Data were obtained from FAO. Population figures are based on estimates from the United Nations.

Fig. 3 Time-series of per capita cereal production for the world, Eastern Africa, Southern Asia, Eastern Asia, and Central America. Values beyond 2007 are projections.

Fig. 4 Multi-model ensemble precipitation changes for the 21st century. These plots show the average change in rainfall for the 21st century, based on a large set of climate change scenarios (Table 2). The output from these simulations was averaged for each season (March-April-May: panel A, June-July-August: panel B, September-October-November: panel C, December-January-February: panel D). Trends over the 2000-2100 time period were then calculated and

plotted. The model simulation shows substantial increases in rainfall over the oceans, which is the only place the models have a meaningful level of skill.

Fig. 5 Summary of our global (PC1, x-axis) and Indian Ocean (IO, y-axis) and precipitation climate change analyses. All indicator time series have been standardized, with an expected mean of zero and standard deviation of 1. Thus a change of +1 would indicate a shift in the mean value equivalent to a 1 standard deviation shift. Each of the four grey dots shows the anticipated seasonal 2050 change for a given season. The inter-model spread of the climate models has been shown using lines spanning a 68% confidence interval.

Fig. 6. The top panel (a) shows the average correlation between the observed and modeled rainfall during the main rainfall season. These seasons are shown with letters, D denotes DJF, M=MAM, J=JJA, S=SON. We show the ensemble correlation, estimated by calculating the correlation for each 20th century model simulation listed in Table 2, and then averaging. The yellow and brown boxes are areas in which modeled rainfall is very inaccurate. The bottom panel (b) shows our estimates of 2050 rainfall changes. These changes are based on the first two principal components of modeled 21st century rainfall, assuming a common CO_2 doubling scenario. These values are based on the main rainy season, and are expressed in standard deviations. The light/dark brown boxes show a modest/considerable reduction in mean rainfall. Results in b reprinted from Brown & Funk (2008), with the permission of AAAS.

Fig. 7 These panels describe our hybrid dynamic-statistical precipitation reformulations for eastern and southern Africa. These reformulations are based on 21st century projections of central Indian Ocean [0-15°S, 60-90°E] precipitation and global precipitation 1st principal components. The left plot shows each location's main growing season (M=MAM, J=JJA, S=SON, D=DJF). The right plot shows downscaled 2050 rainfall projections, expressed as a percent change in main season precipitation. IO and PC1 regression parameters are multiplied by the seasonally appropriate changes shown in Fig. 5. This produces the anticipated change in rainfall.

Fig. 8 Results from our food balance indicator modeling for the Sahel, the Greater Horn of Africa, and Southern Africa. The black bars show historic WFP food aid, accumulated over 13 year intervals. The grey bars show empirical food aid estimates based on regressions with historic agricultural capacity and rainfall (cf. equation 7). The next set of bars show food aid projections based on four different assumptions of future scenarios. The light brown, dark brown, and yellow bars use historic agricultural capacity trends (cf. equation 8) combined with rainfall assumed to either i) trend along observed patterns, ii) trend according to rainfall predicted from Indian Ocean precipitation, or iii) to have no trend at all. The green bars show a scenario based on observed rainfall trends and an agricultural growth scenario.

Fig. 9 Panel (a) shows 2030 yield projections based on historical 1961-2007 trends (cf. Table 3). Values shown before and after arrows denote, respectively, the observed 2007 and projected 2030 per capita cereal production values in kg per person per year. Panel (b) shows targeted yields, assuming the 2030 per capita production values on the right hand sides of the arrows

Bibliography

Adler, R.F., Huffman, G.J., Chang, A., Ferraro, R., Xie, P-P., Janowiak, J., Rudolf, B., Schneider, U., Curtis, S., Bolvin, D., Gruber, A., Susskind, J., Arkin, P., Nelkin, E. (2003). The Version-2 Global Precipitation Climatology Project (GPCP) Monthly Precipitation Analysis (1979-Present). Journal of Hydrometeorology, 4, 1147–1167.

Blaikie, P., Brookfield, H.C. (1987). Land degradation and Society. London: Methuen.

Brown, M.E., Funk, C.C. (2008). Food Security under Climate Change. Science, 319, 580–581.

Cassman, K.G. (2007). Climate change, biofuels, and global food security. Environmental Research Letters 2:doi:10.1088/1748-9326/1082/1081/011002.

Cassman, K.G., Dobermann, A., T.Walters, D., Yang, H. (2003). Meeting Cereal Demand While Protecting Natural Resources and Improving Environmental Quality. Annual Review of Environment and Resources, 28, 315–358.

Chou, C., Tu, J-Y., Tan, P-H. (2007). Asymmetry of tropical precipitation change under global warming. Geophysical Research Letters, 34, L17708.

Davis, C.G., Thomas, C.Y., Amponsah, W.A. (2001). Globalization and Poverty: Lessons from the Theory and Practice of Food Security. American Journal of Agricultural Economics, 83, 714–721.

Devereux, S., Maxwell, S. (2001). Food Security in Sub-Saharan Africa. London: ITDG Publishing.

Fafchamps, M. (2004). Market Institutions in Sub-Saharan Africa: Theory and Evidence. Cambridge, MA: MIT Press.

FAO (2007). The State of Food and Agriculture. Rome, Italy: United Nations Food and Agriculture Organization.

Funk, C., Senay G., Asfaw, A., Korecha, D., Choularton, R., Verdin, J., Eilerts, G., Michaelsen, J. (2005). Recent Rainfall Declines and Food Aid Increases in Ethiopia. Washington, DC: Famine Early Warning Systems Network, USAID.

Funk, C., Dettinger, M.D., Brown, M.E., Michaelsen, J.C., Verdin, J.P., Barlow, M., Hoell, A. (2008). Warming of the Indian Ocean threatens eastern and southern Africa, but could be mitigated by agricultural development. Proceedings of the National Academy of Sciences, 105, 11081–11086.

Funk, C., Verdin J. (2009) Real-time Decision Support Systems: The Famine Early Warning System Network, Ch. 17, Satellite Applications for Surface Hydrology, Springer-Verlag.

Haggblade, S. (2007). Returns to investment in Agriculture. [City]: Michigan State University.

Kates, R.W. (2000). Cautionary tales: Adaptation and the global poor. Climatic Change, 45, 5–17.

Kuhn, T.S. (1962). The Structure of Scientific Revolutions. Chicago: University of Chicago Press.

Lamb, R.L. (2000). Food crops, exports, and the short-run policy response of agriculture in Africa. Agricultural Economics, 22, 271–298.

Lipton, M. (2005). The Family Farm in a Globalizing World: The Role of Crop Science in Alleviating Poverty. Washington, DC: International Food Policy Research Institute.

Lo, H.M., Sene, A. (1989). Human Action and the Desertification of the Sahel. ISSJ, 121, 449–456.

Meehl, G.A., Covey, C., Delworth, T., Latif, M., McAvaney, B., Mitchell, J.F.B., Stouffer, R.J., Taylor, K.E. (2007). THE WCRP CMIP3 Multimodel Dataset: A New Era in Climate Change Research. Bulletin of the American Meteorological Society, 88, 1383–1394.

Naylor, R.L. (1996). Energy and Resource Constraints on Intensive Agricultural Production. Annual Review of Energy and Environment, 21, 99–123.

Parry, M.L., Canziani, O.F., Palutikof, J.P., Linden, P.J., Hanson, C.E. (Eds.) (2007). IPCC (2007) Climate Change 2007: Impacts, Adaptation and Vulnerability. Contribution of Working Group II to the Fourth Assessment Report of the Intergovernmental Panel on Climate Change. Cambridge, UK: Cambridge University Press.

Platteau, J-P. (1996). Physical Infrastructure as a Constraint on Agricultural Growth: The Case of Sub-Saharan Africa. Oxford Development Studies, 24, 189–219.

Rasmusson, E.M. and Carpenter, T.H. (1982) Variations in Tropical Sea Surface Temperature and Surface Wind Fields Associated with the Southern Oscillation/El Niño. Monthly Weather Review 110: 354-384.

Schmidhuber, J., Tubiello, F.N. (2007). Global food security under climate change. Proceedings of the National Academy of Sciences, 104, 19703–19708.

Solomon, S., Qin, D., Manning, M., Marquis, M., Averyt, K., Tignor, M.M.B., Miller, H.L., Chen, Z. (2007). Climate Change 2007 - The Physical Science Basis. Contribution of Working Group I to the Fourth Assessment Report of the IPCC. London: Cambridge University Press.

Turner, B.L., Hyden, G., Kates, R.W. (1993). Beyond Intensification. In B.L. Turner, G. Hyden, R.W. Kates (Eds.), Population Growth and Agricultural Change in Africa. Gainesville: University Press of Florida.

Verdin, J., Funk, C., Senay, G., Choularton, R. (2005a). Climate science and famine early warning. Philosophical Transactions of the Royal Society B: Biological Sciences, 360, 2155–2168.

Verhagen, J., Put, M., Zaal, F., van Keulen, H. (2004). Climate change and Drought Risks for Agriculture. In A.J. Dietz, R. Ruben, A. Verhagen (Eds.), The Impact of Climate Change on Drylands: With a Focus on West Africa (pp. 49–59). Dordrecht, The Netherlands: Kluwer Academic Publishers.

Watts, M. (1989). The Agrarian Question in Africa: Debating the Crisis. Progress in Human Geography, 13, 1–13.

Table 1. Sources of agricultural, social and climate data used in this analysis.

Parameter	*Observed (o) Predicted (p)*	*Time period*	*Source*
Cereal production statistics[a]	o	1961-2007	Food and Agriculture Organisation http://faostat.fao.org/
Population data[b]	o & p	1960-2050	United Nations Population Division http://www.un.org/esa/population/unpop.htm
Annual food aid totals[c]	o	1979-2005	World Food Programme http://www.wfp.org/
Seasonal Rainfall[d]	o	1979-2007	Global Precipitation Climatology Project http://www.gewex.org/gpcp.html
20th and 21st century rainfall simulations	p	1950-2100	Program for Climate Model Diagnosis and Intercomparison http://www-pcmdi.llnl.gov/

[a.] United Nations Food and Agricultural Organisation (FAO) yield, harvested area, seed and fertilizer statistics. These data have been pooled by commodity to include all cereal crops.
[b.] United Nations World Population Division mid-level population estimates and projections.
[c.] Total country level international food aid (food shipments plus cash subsidies), obtained from the FAO database.
[d.] Combined gauge and satellite rainfall estimates, totaled over three-month seasons.
[e.] 20th and 21st climate change change rainfall simulations produced by ten different global climate models.

Table 2. Number of 20th century[a] (1980-2000) & 21st century[b] (2000-2100) simulations used in this study. These model simulations are produced by premier climate modeling groups[c] in the United States, Europe and Asia.

Number of Models	20th Century (1980-2000)	21st century (2000-2100)
GFDL CM 2.1	1	2
GISS ER	4	2
IAP FGOALS	3	3
IPSL CM4	6	1
MIROC3.2 Hi Res	1	1
MIROC3.2 Med Res	3	3
MPI ECHAM5	3	3
MRI CGCM 2.3.2a	1	5
NCAR CCSM 3.0	1	7
UKMO HADGEM1	1	1

[a.] The 20th century simulations are based on observed sea surface temperature and atmospheric aerosol and greenhouse gas patterns, and have been drawn from the Atmospheric Model Intercomparison Project (AMIP) experiment.
[b.] The 21st century simulations are based on predicted a $C0_2$ doubling scenario (SRESA1B) provided by the IPCC. These 21st century climate change simulations are drawn from the World Climate Research Program's Coupled Model Intercomparison Project phase 3 (CMIP3) multi-model dataset (Meehl et al. 2007).
[c.] Simulated 20th and 21st century precipitation fields are drawn from multi-model ensembles of numerical weather predictions obtained from the Programme for Climate Model Diagnostics and Intercomparison. Full details about these models are available at http://www-pcmdi.llnl.gov/projects/cmip/Table.php.

Table 3. This table shows relevant agricultural statistics for 2007 obtained from the FAO. Unless international trade and aid can make up the difference, areas with theoretical food balance deficits will face systematic food shortages. The magnitude of these shortages can be evaluated by looking at the food balance deficits expressed as percentages of the total population. With some exceptions, regions with the largest population increases over the past 27 years also have the largest per capita food deficits.

	Population[a]	Yield[b]	Per capita Harvested Area[c]	Per capita Production[d]	Theoretical Food Balance [millions][e]		% change in population[f]
	Millions of people	kg ha^{-1}	ha person^{-1}	kg person^{-1}	millions of people[e]	[%][f]	[%]
Year(s)	2007	2007	2007	2007	2007	2007	1980-2007
World	6,612	3,347	0.11	354	5,548		49%
Eastern Africa	302	1,482	0.09	131	-96	-32%	107%
Middle Africa	116	967	0.06	62	-79	-68%	113%
Northern Africa	198	1,725	0.11	190	-3	-1%	77%
Southern Africa	54	2,466	0.07	182	-3	-6%	63%
Western Africa	276	1,165	0.16	189	-5	-2%	107%
N. America	337	5,913	0.23	1374	2,066		32%
Cent. America	151	2,893	0.08	243	40		67%
Caribbean	40	2,201	0.02	51	-29	-73%	36%
South America	385	3,704	0.09	349	314		59%
Central Asia	59	1,696	0.32	541	na		11%
Eastern Asia	1,541	5,418	0.06	314	967		31%
Southern Asia	1,603	2,645	0.09	231	323		71%
S-Eastern Asia	570	3,756	0.10	368	518		59%
Western Asia	223	1,985	0.10	204	13		121%
Eastern Europe	295	2,228	0.27	606	632		-18%
N. Europe	96	5,149	0.09	472	140		18%
S. Europe	146	4,147	0.10	416	169		6%
W. Europe	187	6,419	0.09	594	389		9%
Oceania	34	1,221	0.06	68	85		49%

[a.] UN population estimates for 2007.
[b.] The total FAO cereal yield for 2007 for the region.
[c.] The ratio of the total cereals harvested area and population.
[d.] Per capita production, or the ratio of the total cereal production and population.
[e.] The theoretical food balance defined by equation 5. This is the number of unfed people assuming a caloric cereals requirement of 190 kg per person per year.
[f.] Food balance deficits expressed as percentages of the total population in 2007.
[g.] The last column shows recent population increases, expressed a percent of the 1980 population.

Table 4. Global and regional projections of per capita cereal production (equation 1) and theoretical food balance (equation 5) statistics. These values were based on 2030 estimates of yields and per capita harvested area. Overall, and on average for the world, there will be 48 kg less of cereal production per person per year in 2030, a 14% reduction over the 354 kg per person produced in 2007.

	2030 per capita cereal production[a]	Change in annual per capita production (2030 - 2007)		2030 food balance
Units	[kg person^{-1}]	[kg person^{-1}][b]	[%][c]	[Millions][d]
World	306	-48	-14%	4,833
Eastern Africa	84	-47	-36%	-277
Middle Africa	38	-24	-38%	-166
Northern Africa	180	-10	-5%	-18
Southern Africa	189	8	4%	-1
Western Africa	166	-23	-12%	-61
N. America	1,236	-138	-10%	2,168
Cent. America	199	-44	-18%	6
Caribbean	47	-4	-9%	-34
South America	273	-76	-22%	203
Eastern Asia	276	-37	-12%	716
Southern Asia	193	-38	-17%	5
S-Eastern Asia	356	-12	-3%	594
Western Asia	160	-44	-22%	-54
Eastern Europe	542	-64	-11%	468
N. Europe	618	146	31%	227
S. Europe	396	-20	-5%	145
W. Europe	771	176	30%	569
Oceania	1,158	484	72%	213

[a] 2030 yields and per capita harvested area were estimated based on 1960-2007 trends (equations 2-5), and used to derive estimates of 2030 per capita cereal production (equation 1).

[b] The difference, in kilograms per person, between projected 2030 and observed 2007 per capita cereal production.

[c] The difference, expressed as a percentage change, between projected 2030 and observed 2007 per capita cereal production.

[d] theoretical food balance (eq. 2) for 2030, expressed in millions of people, based on an annual cereal requirement of 190 kg person^{-1} year^{-1}.

Table 5. Selected African agriculture and population statistics from the FAO.

	Change in pop. w.o. food[a] 2007 minus 1980 [thousands]	Change in WFP food aid[b] 2007 minus 1980 [kilotonnes]	Rainfall Change[c] 92-05 vs. 79-91,[%]	Change in pop.[d] 2005 minus 1979 [millions]	Per cap agric. capacity[e], 1979	Per cap agric. capacity[e], 2005	Per cap harvested area[f], 1979	Per cap harvested area[f], 2005	Fertilizer use[g] [kg ha^{-1}] 1979	Fertilizer use[g] [kg ha^{-1}] 2005	Ag. Capacity Trend[h] 1994-2005 [kg person^{-1} year^{-2}]
Zimbabwe	1,126	171	-6%	6	228	117	0.19	0.13	85	66	-3
Zambia	646	-17	-5%	5	221	126	0.11	0.08	94	76	-2
Swaziland	70	9	4%	1	178	108	0.13	0.06	193	114	-3
Lesotho	-41	-6	13%	1	255	245	0.16	0.15	22	43	6
Malawi	516	74	-3%	7	191	137	0.21	0.13	20	26	2
Mozambique	183	-12	2%	8	68	100	0.08	0.11	24	12	2
Tanzania	1,338	114	-13%	20	145	125	0.15	0.09	11	0	2
Kenya	1,339	48	-13%	16	147	116	0.12	0.07	21	67	0
Ethiopia/Eritrea	3,064	796	-12%	37	139	121	0.12	0.11	8	19	-2
Uganda	1,621	134	1%	15	53	56	0.07	0.06	0	4	-1
Rwanda	570	21	-3%	4	49	31	0.05	0.04	1	1	0
Burundi	470	49	-7%	3	41	26	0.05	0.03	5	12	0
Niger	271	22	16%	7	222	170	0.68	0.52	0	1	-5
Mali	-169	-53	8%	7	181	199	0.21	0.27	11	12	2
Senegal	704	-87	2%	5	240	133	0.20	0.11	27	28	-2
Mauritania	170	-26	16%	2	162	106	0.08	0.05	17	20	-4
Burkina Faso	-695	-24	5%	7	140	209	0.31	0.22	0	1	4
Chad	-48	1	4%	5	216	203	0.25	0.20	0	10	-2

[a] The difference in the theoretical population without food (equation 5) calculated with 2007 and 1980 data.
[b] The difference WFP food aid in 2007 and 1980.
[c] The change in main growing season rainfall, averaged over 1992-2005 and 1979-1991, expressed as a percent of the 1979-2005 mean.
[d] The change in total population between 2005 and 1979, expressed in millions.
[e] Per capita agricultural capacity (h) as defined by equation 8, with units of kg of cereal production per person per year, based on FAO statistics.
[f] Per capita harvested area, based on FAO statistics.
[g] Per hectare fertilizer use, based on FAO statistics.
[h] Annual change (trend) in per capita agricultural capacity (h, equation 8), in kg of cereal production per person per year per year.

Figures

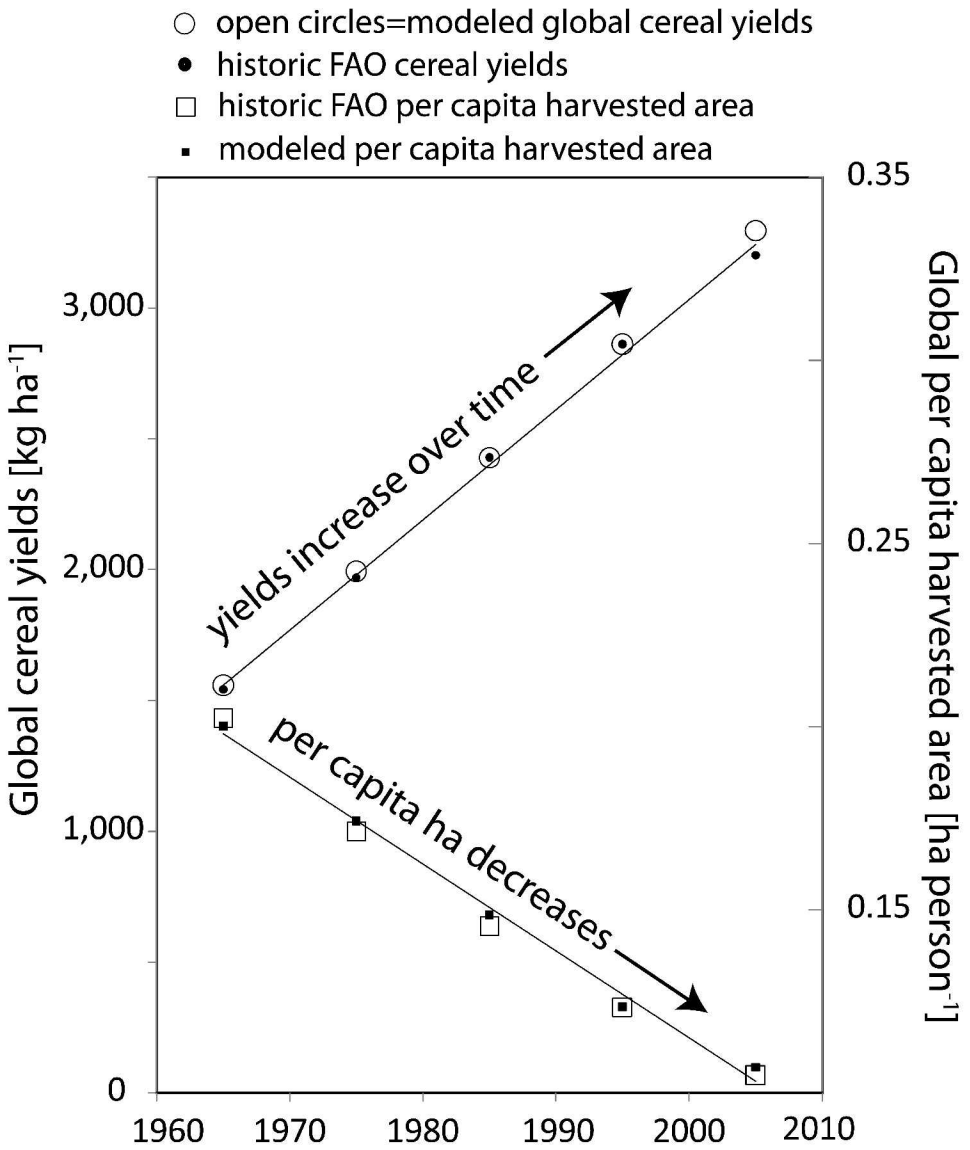

Fig. 1 Oberserved (FAO) and modeled global cereal trends in per capita harvested area and yields. Data values have been averaged by decades. The filled circles show observed global cereal yields. Decadal increases in global yields are fit very well by a linear trend model (filled circles). The open boxes show observed per capita harvested area decreases. Decadal decreases in global per capita harvested areas are also fit very well by a linear trend model (filled boxes). The relative rates of yield increases and per capita harvested area decreases can be used to predict future per capita cereal production.

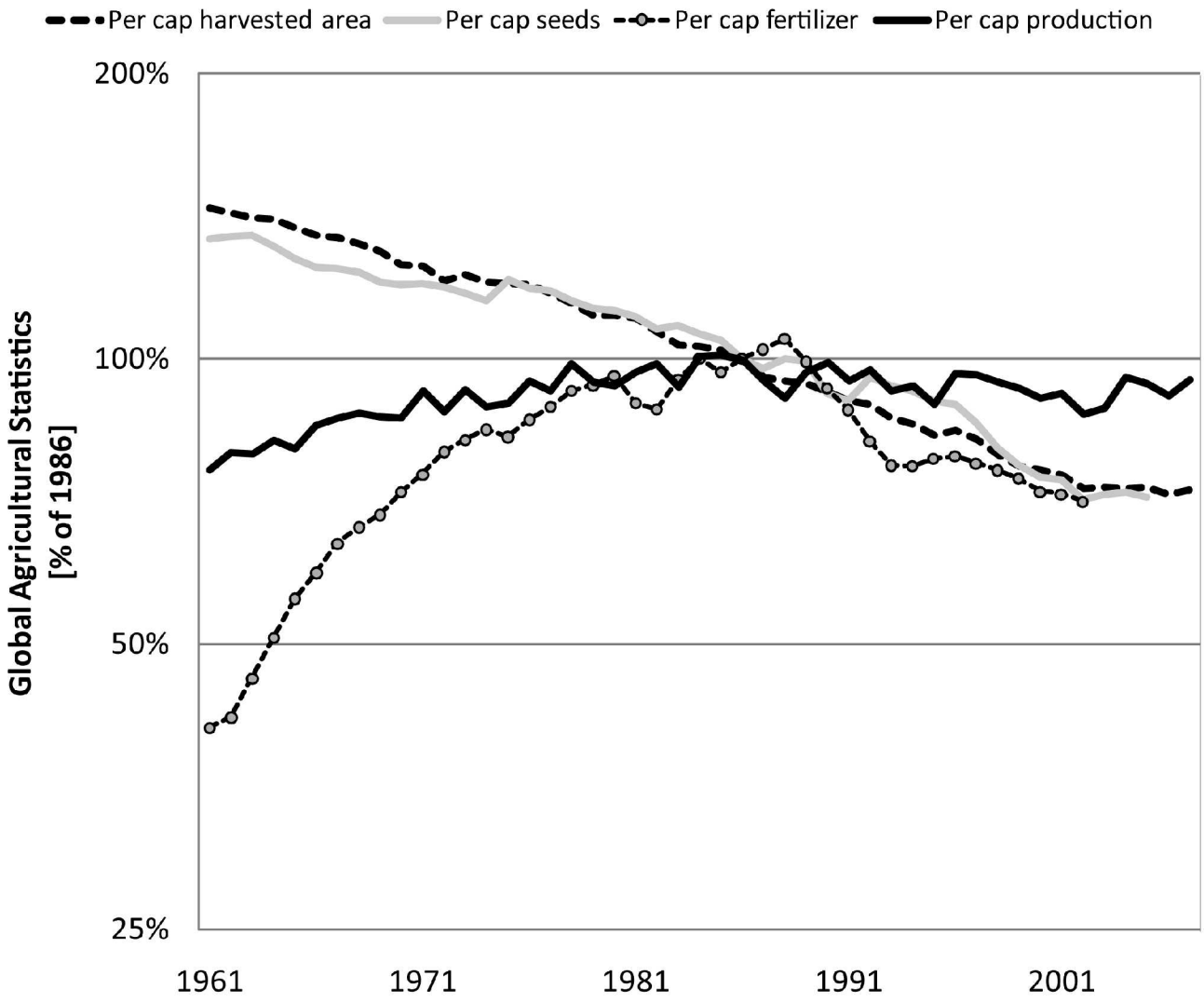

Fig. 2 Global per capita cereal production statistics, expressed as fractions of a 1986 baseline. Data were obtained from FAO. Population figures are based on estimates from the United Nations.

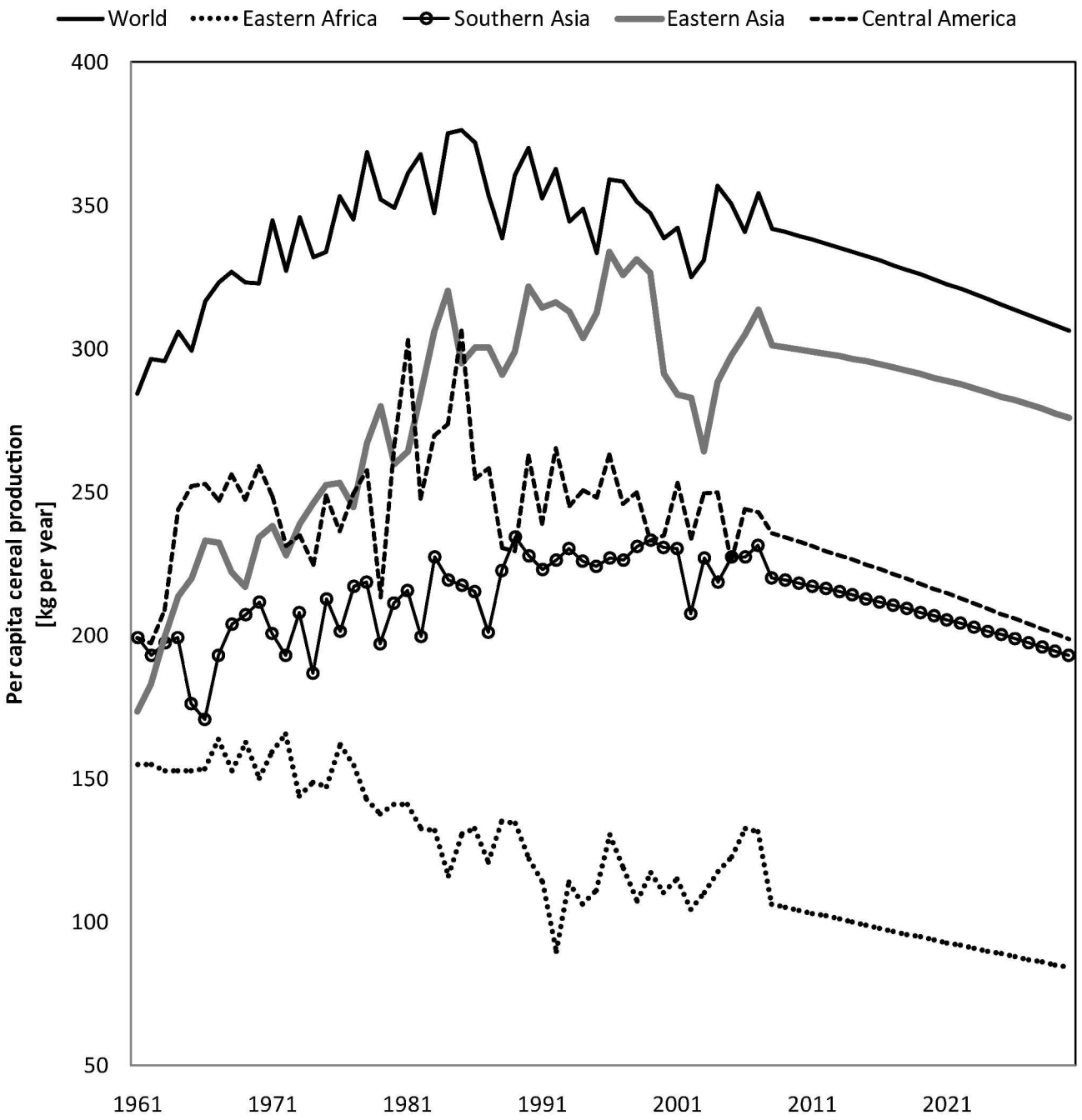

Fig. 3 Time-series of per capita cereal production for the world, Eastern Africa, Southern Asia, Eastern Asia, and Central America. Values beyond 2007 are projections.

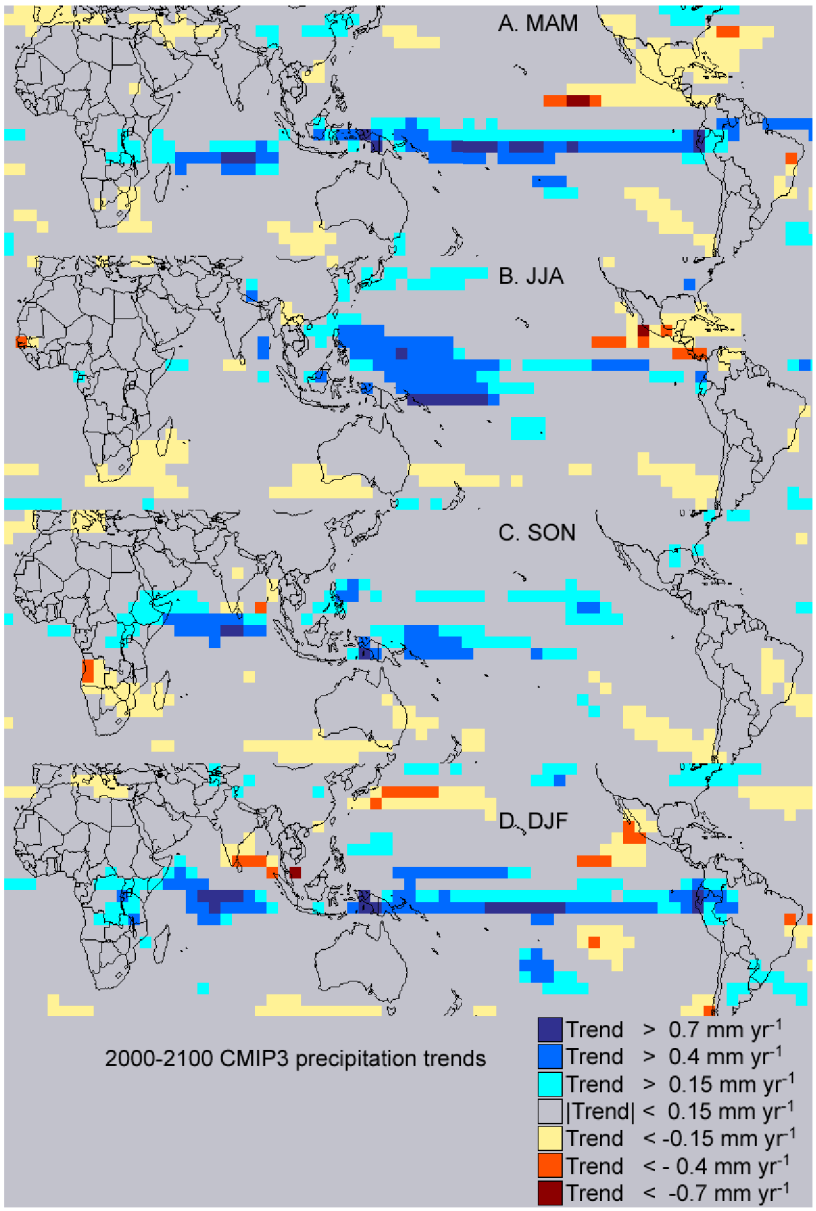

Fig. 4 Multi-model ensemble precipitation changes for the 21st century. These plots show the average change in rainfall for the 21st century, based on a large set of climate change scenarios (Table 2). The output from these simulations was averaged for each season (March-April-May: panel A, June-July-August: panel B, September-October-November: panel C, December-January-February: panel D). Trends over the 2000-2100 time period were then calculated and plotted. The model simulation shows substantial increases in rainfall over the oceans, which is the only place the models have a meaningful level of skill.

Fig. 5 Summary of our global (PC1, x-axis) and Indian Ocean (IO, y-axis) and precipitation climate change analyses. All indicator time series have been standardized, with an expected mean of zero and standard deviation of 1. Thus a change of +1 would indicate a shift in the mean value equivalent to a 1 standard deviation shift. Each of the four grey dots shows the anticipated seasonal 2050 change for a given season. The inter-model spread of the climate models has been shown using lines spanning a 68% confidence interval.

a. Average correlation between simulated and observed main season rainfall, 1980-2000

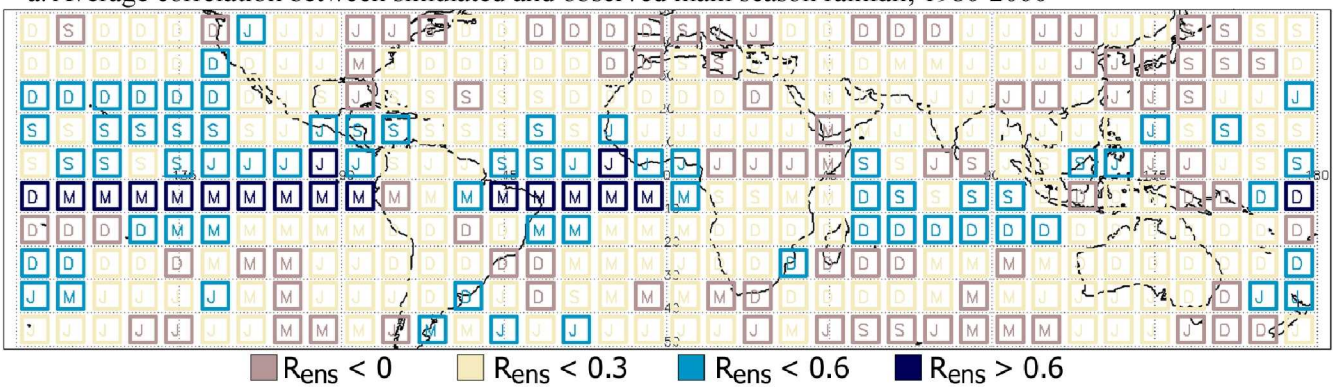

b. Statistical estimates of 2050 main season rainfall changes, expressed in standard deviations

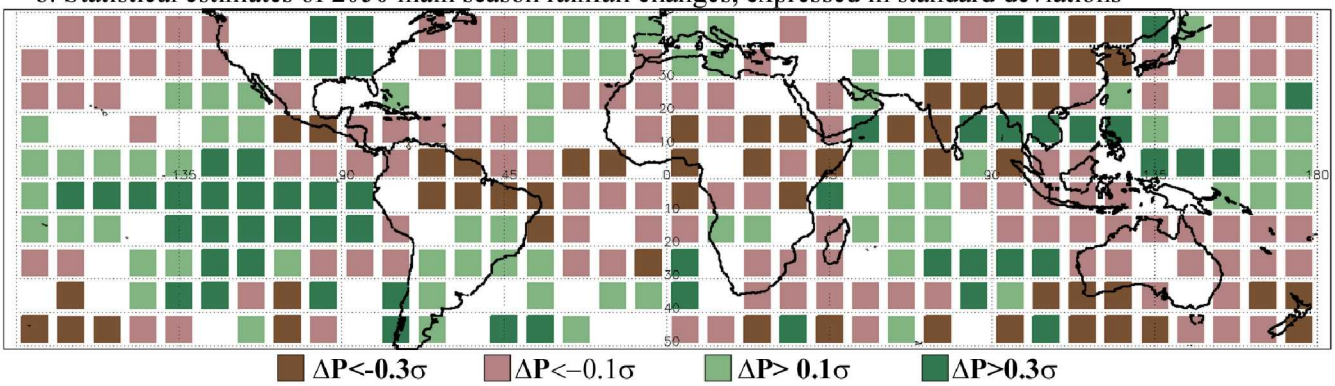

Fig. 6. The top panel (a) shows the average correlation between the observed and modeled rainfall during the main rainfall season. These seasons are shown with letters, D denotes DJF, M=MAM, J=JJA, S=SON. We show the ensemble correlation, estimated by calculating the correlation for each 20th century model simulation listed in Table 2, and then averaging. The yellow and brown boxes are areas in which modeled rainfall is very inaccurate. The bottom panel (b) shows our estimates of 2050 rainfall changes. These changes are based on the first two principal components of modeled 21st century rainfall, assuming a common CO_2 doubling scenario. These values are based on the main rainy season, and are expressed in standard deviations. The light/dark brown boxes show a modest/considerable reduction in mean rainfall. Results in b reprinted from Brown & Funk (2008), with the permission of AAAS.

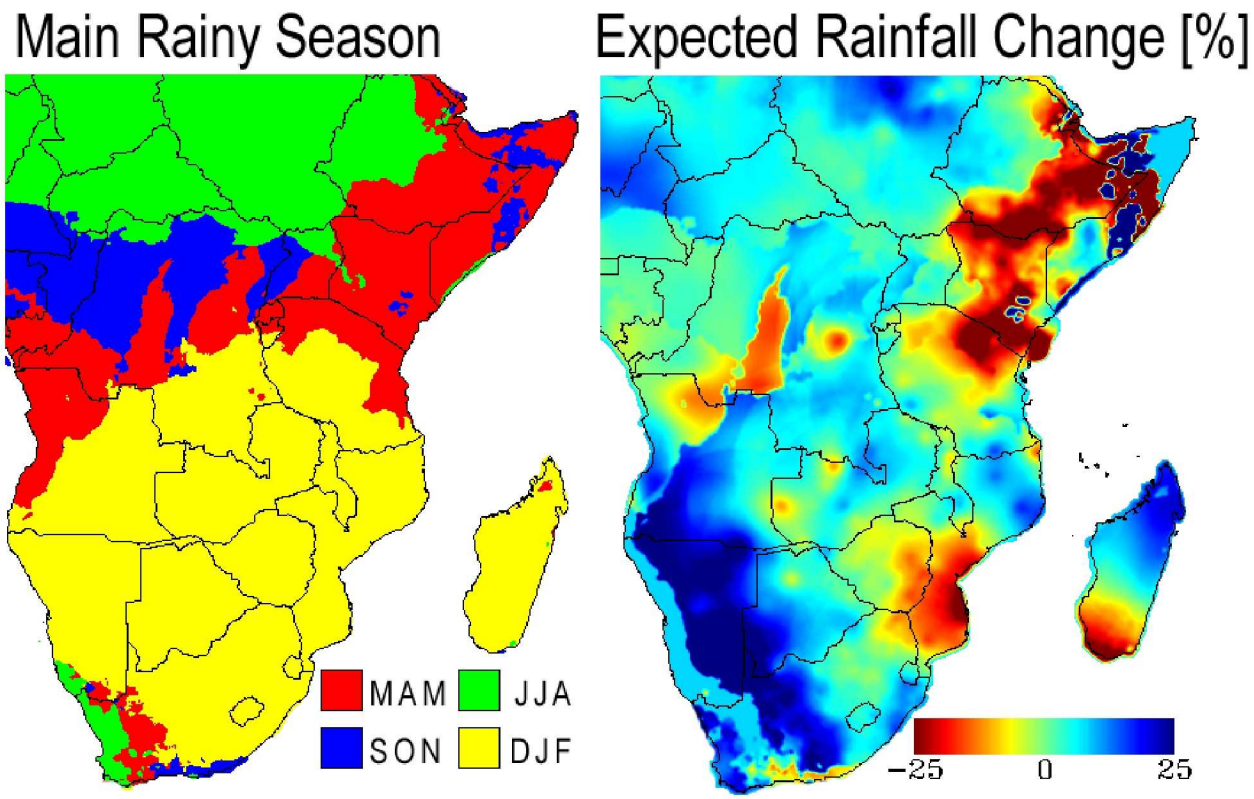

Fig. 7 These panels describe our hybrid dynamic-statistical precipitation reformulations for eastern and southern Africa. These reformulations are based on 21st century projections of central Indian Ocean [0-15°S, 60-90°E] precipitation and global precipitation 1st principal components. The left plot shows each location's main growing season (M=MAM, J=JJA, S=SON, D=DJF). The right plot shows downscaled 2050 rainfall projections, expressed as a percent change in main season precipitation. IO and PC1 regression parameters are multiplied by the seasonally appropriate changes shown in Fig. 5. This produces the anticipated change in rainfall.

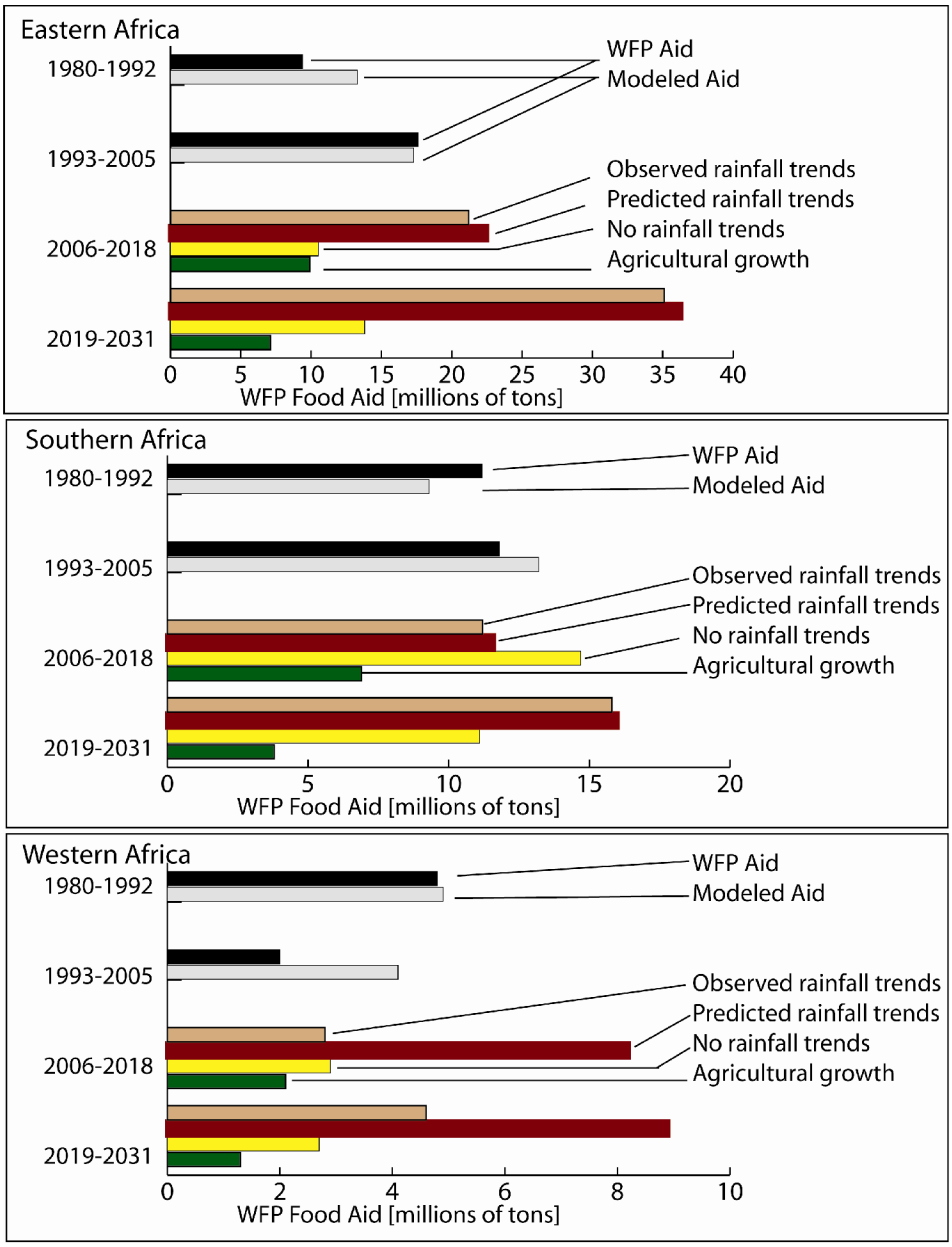

Fig. 8 Results from our food balance indicator modeling for the Sahel, the Greater Horn of Africa, and Southern Africa. The black bars show historic WFP food aid, accumulated over 13 year intervals. The grey bars show empirical food aid estimates based on regressions with historic agricultural capacity and rainfall (cf. equation 7). The next set of bars show food aid projections based on four different assumptions of future scenarios. The light brown, dark brown, and yellow bars use historic agricultural capacity trends (cf. equation 8) combined with rainfall assumed to either i) trend along observed patterns, ii) trend according to rainfall predicted from Indian Ocean precipitation, or iii) to have no trend at all. The green bars show a scenario based on observed rainfall trends and an agricultural growth scenario.

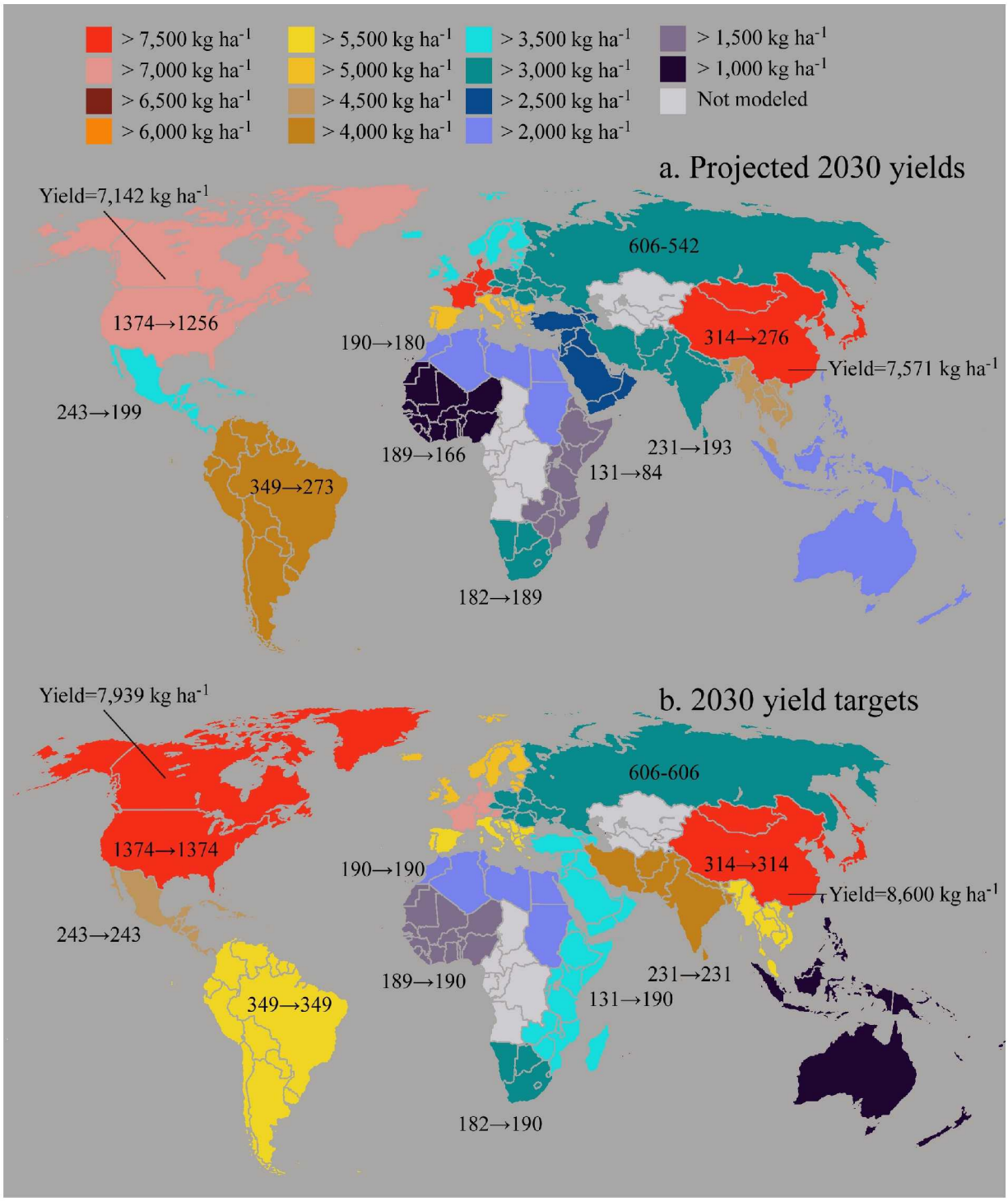

Fig. 9 Panel (a) shows 2030 yield projections based on historical 1961-2007 trends (cf. Table 3). Values shown before and after arrows denote, respectively, the observed 2007 and projected 2030 per capita cereal production values in kg per person per year. Panel (b) shows targeted yields, assuming the 2030 per capita production values on the right hand sides of the arrows